ICIC Express Letters
Part B: Applications
Volume **9**, Number **7**, July **2018**

ICIC International ©2018 ISSN 2185-2766
pp. **673–680**

EFFECTS OF FLOW ASYMMETRICITY ON THROMBUS FORMATION AND HEMOLYSIS PROPERTIES IN THE PIPE ORIFICE FLOW BY CFD ANALYSIS

Chiharu Hirayama, Yuko Miyamura and Masaaki Tamagawa

Graduate School of Life Science and Systems Engineering
Kyushu Institute of Technology
Hibikino 2-4, Wakamatsu-ku, Kitakyushu, Fukuoka 808-0196, Japan
cosmonaut_no1@yahoo.co.jp; miyamura.yuko835@mail.kyutech.jp; tama@life.kyutech.ac.jp

Received January 2018; accepted April 2018

Abstract. *In this paper, to discuss asymmetricity of the thrombus formation on the wall surface, flow analysis on the three-dimensional flow in the pipe orifice was carried out, and the effects of asymmetricity of wall shear stress and shear stress on thrombus formation and hemolysis properties were investigated. As for thrombus formation, the asymmetricity of wall shear stress was obtained and compared with that of visualization of thrombus formation. As for hemolysis properties on orifice flows, it was evaluated by Lagrangian fatigue accumulation method in case of axisymmetric flow and three-dimensional flow. From the results, it was suggested that there is the possibility for wall shear stress and other transport process of concentration to influence circumferential thrombus formation. In addition to this, by comparing the hemolysis evaluation of the axisymmetric flow with the three-dimensional flow, it was also suggested that the flow asymmetricity has effects on hemolysis properties by comparing with axisymmetric flow.*
Keywords: Flow asymmetricity, Thrombus formation, Hemolysis, Shear stress

1. **Introduction.** Recently design and development of medical fluidics including artificial hearts, artificial valves and stent have been world-widely investigated, but the hemolysis and the thrombus formation occurring in these devices are serious problems [1-4]. It is still now necessary to predict the shear stress in the fluidics as shear stress is involved in these phenomena [5-8].

In our previous investigation [9], to find out the correlation between flow field and thrombus formation on shear flows in the orifice pipe generating high shear rate, visualization of thrombus formation and Computational Fluid Dynamics (CFD) analysis were done. In the previous visualization of thrombus formation, the thrombus formation rate in the circumferential direction on the wall surface of the orifice pipe was measured, and it was found that direction of thrombus formation on the wall surface was asymmetric. However, the evaluation for this asymmetricity has not been established yet. In the previous CFD analysis, flow analysis on the pipe orifice flow was carried out and the flow field data was obtained in detail. However, this analysis was dealt as an axisymmetric one, and it was difficult to find out the correlation between flow field and thrombus formation by comparing directly with the visualization of thrombus formation.

By the way, from the fluid mechanical points of view, it is an interesting topic to find out the relation between flow asymmetricity [10] and asymmetricity of thrombus formation. In this investigation, to discuss asymmetricity of the thrombus formation on the wall surface, flow analysis on the three-dimensional flow in the pipe orifice was carried out, and the effects of asymmetricity of wall shear stress and shear stress on thrombus formation and hemolysis properties were investigated. The key point of this investigation

DOI: 10.24507/icicelb.09.07.673

is that thrombus and hemolysis are induced by shear stress in the flow or on the wall (wall shear stress).

In this paper, the computational objects and methods of axisymmetric flow and three-dimensional flow in the orifice are described in Section 2, and the results and related matters are discussed using computer simulations of axisymmetric flow and three-dimensional flow in Section 3. And the result of asymmetricity for three-dimensional flow is compared with that of distribution of thrombus formation by experiments. In addition, the hemolysis evaluation between axisymmetric flow and three-dimensional flow are investigated and discussed. In Section 4, concluding remarks are described.

2. **Computational Objects and Methods.**

2.1. **Computational objects.** In this computation, the orifice pipe of two geometries (AB, BB) with the internal diameter $D = 22$ [mm] and the diameter of contraction part $d = 8$ [mm] shown in Figure 1 are used. Using these geometries, the previous results of axisymmetric analysis of the orifice pipe are compared with the three-dimensional analysis result of the same orifice pipe flow.

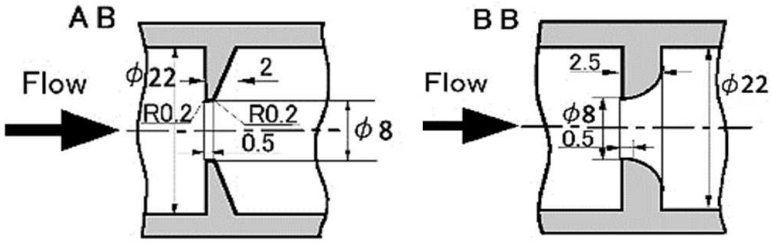

FIGURE 1. Geometries of orifices

2.2. **Computational method.**

2.2.1. *Axisymmetric flow.* As for governing equations of the axisymmetric flow in the orifice pipe, a continuity equation and Navier-Stokes equations are used as follows:

$$\frac{\partial u}{\partial x} + \frac{1}{r}\frac{\partial (rv)}{\partial r} = 0 \tag{1}$$

$$\frac{\partial u}{\partial t} + u\frac{\partial u}{\partial x} + v\frac{\partial v}{\partial r} = -\frac{\partial p}{\partial x} + \left(\frac{1}{Re} + \nu_t\right)\nabla^2 u + 2\frac{\partial \nu_t}{\partial t}\frac{\partial u}{\partial x} + \frac{\partial \nu_t}{\partial r}\left(\frac{\partial u}{\partial r} + \frac{\partial v}{\partial x}\right) \tag{2}$$

$$\frac{\partial v}{\partial t} + u\frac{\partial v}{\partial x} + v\frac{\partial v}{\partial r} = -\frac{\partial p}{\partial r} + \left(\frac{1}{Re} + \nu_t\right)\left(\nabla^2 v - \frac{v}{r^2}\right) + 2\frac{\partial \nu_t}{\partial t}\frac{\partial v}{\partial r} + \frac{\partial \nu_t}{\partial x}\left(\frac{\partial u}{\partial r} + \frac{\partial v}{\partial x}\right) \tag{3}$$

where r, x indicate coordinate of radial and flow axis, u, v indicate velocity of each direction, p is pressure, ν is dynamic viscosity, ν_t is turbulent viscosity, and Re means Reynolds number.

In addition to this, as the flow in the pipe is a fully developed turbulent flow in all regions except the wall surface, k-ε equations (k: turbulent energy, ε: energy dissipation) with the modified Lounder-Kato model are used as follows:

$$\frac{\partial k}{\partial t} + u\frac{\partial k}{\partial x} + v\frac{\partial k}{\partial r} = \frac{1}{Re}\nabla^2 k + \frac{1}{\sigma_k}\left(\frac{\partial \nu_t}{\partial x}\frac{\partial k}{\partial x} + \frac{\partial \nu_t}{\partial r}\frac{\partial k}{\partial r}\right) + G - \varepsilon \tag{4}$$

$$\frac{\partial \varepsilon}{\partial t} + u\frac{\partial \varepsilon}{\partial x} + v\frac{\partial \varepsilon}{\partial r} = \frac{1}{Re}\nabla^2 \varepsilon + \frac{1}{\sigma_\varepsilon}\left(\frac{\partial \nu_t}{\partial x}\frac{\partial \varepsilon}{\partial x} + \frac{\partial \nu_t}{\partial r}\frac{\partial \varepsilon}{\partial r}\right) + C_{\varepsilon 1}\frac{\varepsilon}{k}G - C_{\varepsilon 2}f_\varepsilon\frac{\varepsilon^2}{k} \tag{5}$$

$$\nu_t = C_\mu f_\mu \frac{k^2}{\varepsilon} \tag{6}$$

where $C_\mu = 0.09$, $C_{\varepsilon 1} = 1.5$, $C_{\varepsilon 2} = 1.9$, $\sigma_k = 1.4$, $\sigma_\varepsilon = 1.4$, and f_μ, f_ε show the damping functions near the wall for low Reynolds number model, and G means generation term.

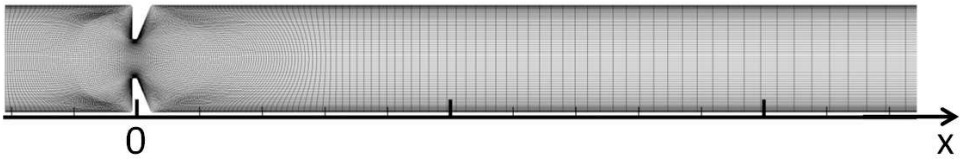

FIGURE 2. Computational mesh of axisymmetric orifice

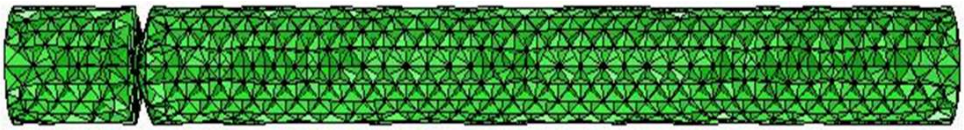

FIGURE 3. Computational mesh of three-dimensional orifice

Figure 2 shows typical mesh distribution of the axisymmetric orifice (200×50 points). As for the boundary conditions, it is fully developed velocity with flow rate 5 [L/min] at the inlet, velocity gradient = 0 and pressure = 0 [Pa] at the outlet. No-slip condition is given to the wall. Regarding the turbulent quantity, 5% disturbance of the inflow velocity is added. Assuming that plasma flows, physical properties of plasma viscosity 1.2×10^{-3} [Pa·s] and density 1.03×10^3 [kg/m^3] were used.

2.2.2. *Three-dimensional flow.* Concerning about the 3D analysis, the 3-diemsional continuity equation and Navier-Stokes equations, and k-ω equations with SST model are used. As for the flow analysis in the three-dimensional flow, the thermal fluid analysis code (ANSYS FLUENT 17.2) is used. Figure 3 shows typical mesh of three-dimensional flow, and the computation mesh generated by ICEM CFD in ANSYS FLUENT is tetrahedral type.

2.2.3. *Evaluation method for hemolysis.* Based on the method of Giersiepen et al. [11], hemolysis in the orifice flow is evaluated. The hemolysis evaluation quantity EST is defined as follows:

$$EST = \int_V d_m \cdot U dV \tag{7}$$

where U $(= \sqrt{u^2 + v^2})$ is the total flow velocity, and V is the calculated volume. And d_m is the degree of damage, which is function of the shear stress τ received by the erythrocyte from the flow field and its duration time t. This d_m is expressed as follows:

$$d_m = 3.62 \times 10^{-7} \cdot \tau^{2.416} \cdot \Delta t^{0.785} \tag{8}$$

where τ, Δt indicate shear stress and duration time of passing through a computational cell. From Equation (7) and Equation (8), the following evaluation quantity EST is derived.

$$EST = 3.62 \times 10^{-7} \int_V \tau^{2.416} \cdot \Delta t^{0.785} \cdot \sqrt{u^2 + v^2} dV \tag{9}$$

Using the flow fields, the damage of red blood damage is evaluated by this EST.

3. **Results and Discussions.**

3.1. **Comparison between axisymmetric flow and three-dimensional flow.** Figure 4 shows the streamlines in the axisymmetric orifice flow, and Figure 5 shows the particle path in the three-dimensional orifice flow. From Figure 4, it is confirmed that there is a reattachment point at the position of $x = 5.6$ cm in the axisymmetric orifice flow. However, in the three-dimensional flow, there are variations from the position of

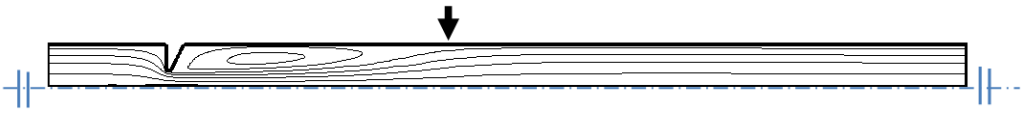

FIGURE 4. Streamline in case of axisymmetric orifice flow (Arrow shows reattachment point of the flow)

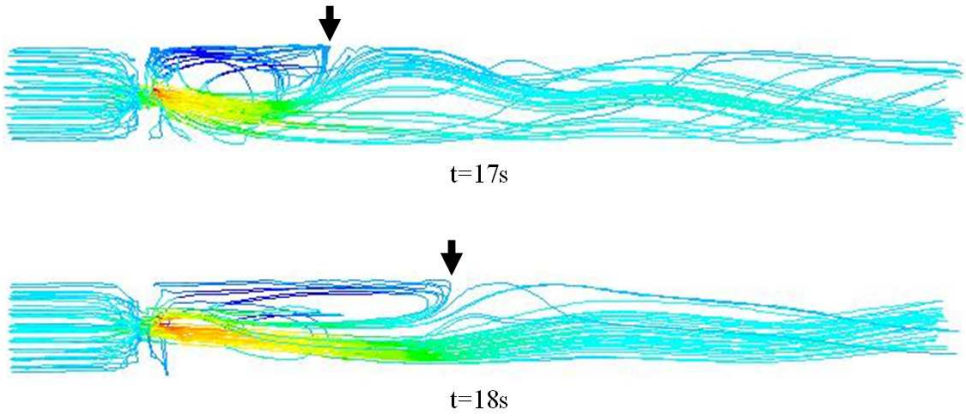

FIGURE 5. Path line in case of three-dimensional orifice flow (Arrows show reattachment point of the flow)

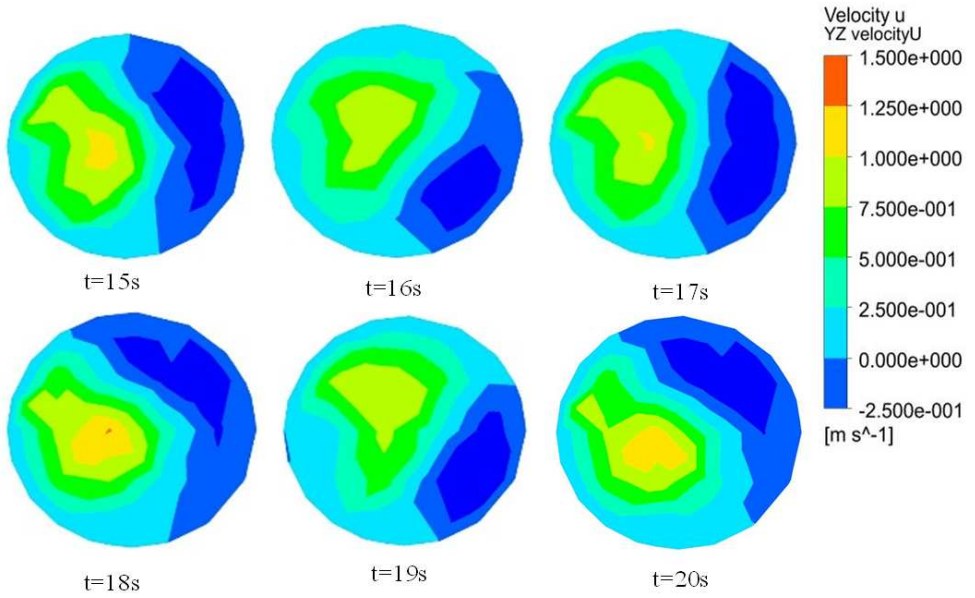

FIGURE 6. Contour of velocity u with time ($x = 19.8$ mm)

the reattachment point at each time. Furthermore, it is also found that there should be asymmetry for the path line itself.

Figure 6 shows the time history of the contour plot of the flow direction velocity as viewed from the y-z plane ($x = 1.98$ cm). From this figure, it is also confirmed that there should be flow asymmetry, and it is found that the position of the vortex is fluctuating with time.

3.2. **Distribution of wall shear stress in θ direction.** Figure 7 shows distributions of wall shear stress of geometries AB and BB. Figure 8 shows the θ direction distribution of wall shear stress in the cross section of these contour plots at proper point. From Figure 7 and Figure 8, it is found that wall shear stress is asymmetrically distributed in both geometries AB and BB.

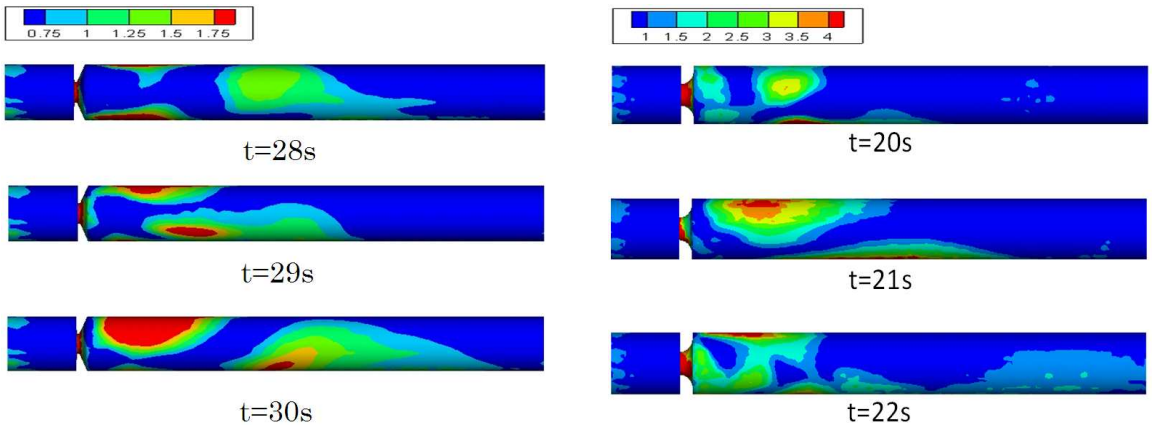

(a) Orifice AB (b) Orifice BB

FIGURE 7. Wall shear stress in case of three-dimensional orifice flow

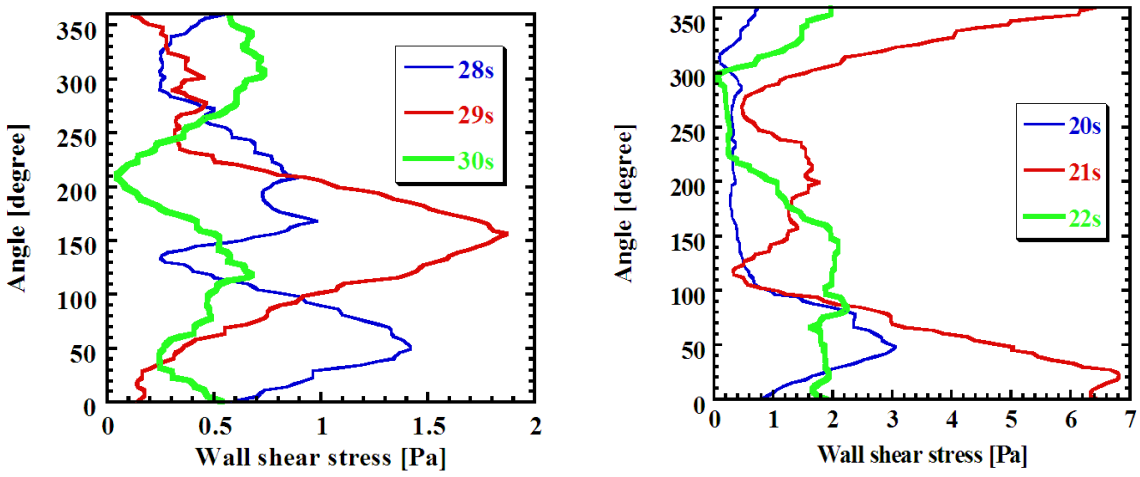

(a) Orifice AB (b) Orifice BB

FIGURE 8. Distribution of wall shear stress on θ direction for orifice AB and BB

3.3. **Evaluation of flow asymmetricity and thrombus formation on the wall surface.** Figure 9(a) shows a schematics of an experimental apparatus for visualization experiment of thrombus formation conducted in the previous investigations. Figure 9(b) shows an image obtained by image processing of thrombus formation with a CCD camera. The white part behind the orifice pipe in this figure shows a white thrombus. It is shown that the white thrombus is spreading asymmetrically.

Figure 10 shows definition of variation and mean value of wall shear stress for the θ direction distribution. In this figure, the distribution in the x direction (flow direction) of the variation width of wall shear stress is shown. The variation range is defined as the ratio of the width of wall shear stress ($\Delta\tau_{w,p\text{-}p}$) to the average value with circumferential angle ($\tau_{w,m}$). It means that the wall shear stress is considered to be symmetric when this value is 0.

Figure 11 shows relationship between normalized variation of wall shear stress and position x in case of orifice BB and AB. In this figure, typical distribution of thrombus formation for orifice BB is also shown. As there are not so many samples of thrombus images for orifice AB, only the results of orifice BB are shown here. Although there are no data for orifice AB, it is discussed whether the normalized variation of wall shear stress contributes to asymmetricity of thrombus formation by comparing with the experimental results or not.

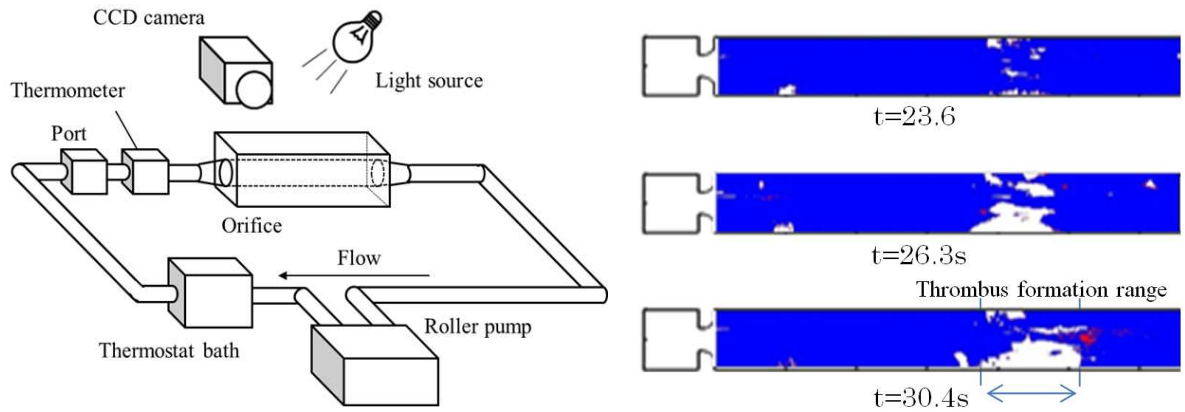

(a) Experimental apparatus for thrombus observation

(b) Propagation of white thrombus formation on the wall (Orifice BB)

FIGURE 9. Visualization of thrombus formation on the surface (previous experiments [9])

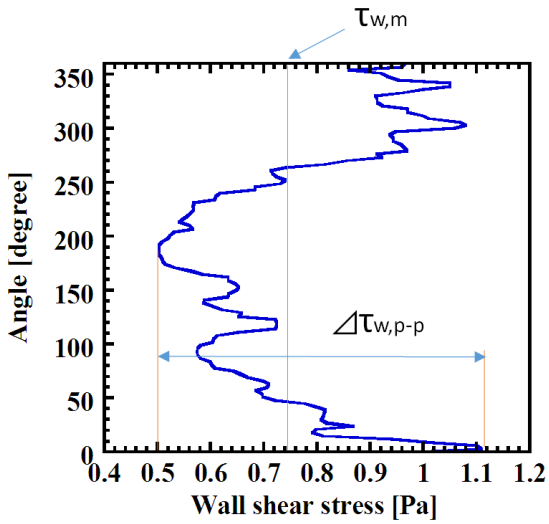

FIGURE 10. Definition of variation and mean value of wall shear stress

From Figure 11, it is not clearly found that there are strong correlations between normalized variation of wall shear stress and asymmetric distribution of white thrombus in case of orifice BB. In this figure, there is the maximum point of normalized variation at $x = 7.5$ (cm), and this position corresponds to the reattachment point of the flow at the wall. So it is necessary to consider both the transport process of concentration of platelet or coagulation factor and this normalized variation of wall shear stress. It is suggested that both of them have effects on asymmetricity of thrombus formation.

3.4. **Evaluation of hemolysis and flow asymmetricity.** Figure 12 shows time history of the hemolysis evaluation *EST* of the axisymmetric flow and the three-dimensional flow in the orifice BB. In this figure, only the result of orifice BB is shown as same as in the previous subsection. The red line shows the case of axisymmetric flow, the blue line (solid line) shows the case of three-dimensional flow, and the dashed line shows the time-averaged value of the three-dimensional flow. From this figure, it is clearly found that the periodic variation occurs in the three-dimensional flow, but the time-averaged value has almost the same value as the axisymmetric flow. Then it is found that it is possible to predict hemolysis properties with considering variation of shear stress by using the

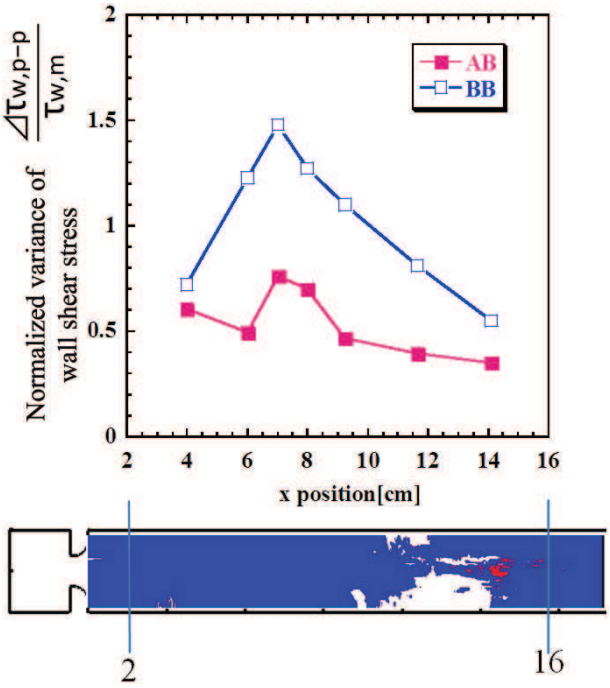

FIGURE 11. Relationships between normalized variation of wall shear stress and position x (Orifice BB)

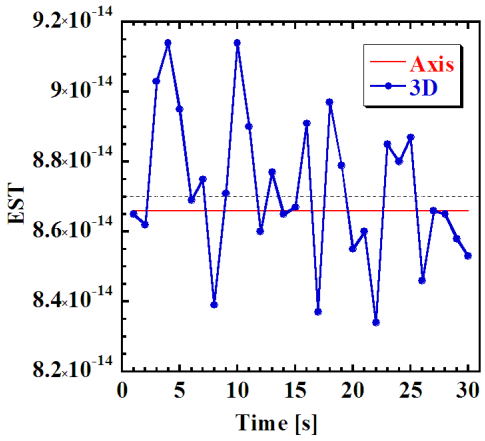

FIGURE 12. Time history of evaluation of hemolysis in orifice BB (Dashed line: mean value)

evaluation value *EST* of the three-dimensional flow. To establish the accurate prediction method of hemolysis properties, it is necessary to get more data by experiments in vitro.

4. **Conclusions.** To discuss asymmetricity of the thrombus formation on the wall surface, flow analysis on the three-dimensional flow in the pipe orifice was carried out, and the effects of asymmetricity of wall shear stress and shear stress on thrombus formation and hemolysis properties were investigated. The following matters are concluded as follows.

1) Asymmetricity of the wall shear stress was obtained in the flow of the three-dimensional flow, and it was suggested that there is the possibility for wall shear stress and other transport process of concentration to influence circumferential thrombus formation.

2) Asymmetricity of the flow has effects on hemolysis properties by comparing with axisymmetric flow.

Further experiments for this validation will be needed to establish the evaluation method related to asymmetricity of thrombus formation and hemolysis properties.

Acknowledgment. A part of this work was supported by Grant-in-Aid for Scientific Research on Innovative Areas 15H01601, and Challenging Research (Exploratory) 17K18844.

REFERENCES

[1] T. Akamatsu, T. Tsukiya, K. Nishimura, C. H. Park and T. Nakazeki, Recent studies of the centrifugal blood pump with a magnetically suspended impeller, *Artificial Organs*, vol.19, no.7, pp.631-634, 1995.

[2] T. Shigemitsu, J. Fukutomi, T. Wada and H. Shinohara, Performance analysis of mini centrifugal pump with splitter blades, *Journal of Thermal Science*, vol.22, no.6, pp.537-579, 2013.

[3] U. Morbiducci, R. Ponzini, M. Nobili, D. Massai, F. M. Montevecchi, D. Bluestein and A. Redaelli, Blood damage safety of prosthetic heart valves. Shear-induced platelet activation and local flow dynamics: A fluid-structure interaction approach, *Journal of Biomechanics*, vol.42, no.12, pp.1952-1960, 2009.

[4] F. M. Susin, S. Espa, R. Toninato, S. Fortini and G. Querzoli, Integrated strategy for in vitro characterization of a bileaflet mechanical aortic valve, *Biomed. Eng. Online*, vol.16, no.1, p.29, 2017.

[5] S. C. Shadden and A. Arzani, Lagrangian postprocessing of computational hemodynamics, *Ann. Biomed. Eng.*, vol.43, no.1, pp.41-58, 2015.

[6] R. A. Malinauskas, P. Hariharan, S. W. Day, L. H. Herbertson, M. Buesen, U. Steinseifer, K. I. Aycock, B. C. Good, S. Deutsch, K. B. Manning and B. A. Craven, FDA benchmark medical device flow models for CFD validation, *ASAIO J.*, vol.63, no.2, pp.150-160, 2017.

[7] Z. Xu, J. Lioi, J. Mu, M. M. Kamocka, X. Liu, D. Z. Chen, E. D. Rosen and M. Alber, A multiscale model of venous thrombus formation with surface-mediated control of blood coagulation cascade, *Biophysical Journal*, vol.98, pp.1723-1732, 2010.

[8] G. Moiseyev, S. Givli and P. Z. Bar-Yoseph, Fibrin polymerization in blood coagulation – A statistical model, *Journal of Biomechanics*, vol.46, pp.26-30, 2013.

[9] Y. Yi, M. Tamagawa and W. Shi, Prediction of thrombus formation on the wall by high shear rate on couette and orifice blood flows, *Journal of Medical Imaging and Health Informatics*, vol.7, no.1, pp.79-84, 2017.

[10] S. J. Sherwin and H. M. Blackburn, Three-dimensional instabilities and transition of steady and pulsatile axisymmetric stenotic flows, *Journal of Fluid Mechanics*, vol.533, pp.297-327, 2005.

[11] M. Giersiepen, L. J. Wurzinger, R. Opitz and H. Reul, Estimation of shear stressrelated blood damage in heart valve prostheses – In vitro comparison of 25 aortic valves, *International Journal of Artificial Organs*, vol.13, no.5, pp.300-306, 1990.